X-ray excited optical luminescence, photoluminescence, photostimulated luminescence and x-ray photoemission spectroscopy studies on BaFBr:Eu

1997 J. Phys.: Condens. Matter 9 4769

(http://iopscience.iop.org/0953-8984/9/22/027)

J. Phys.: Condens. Matter **9** (1997) 4769–4780. Printed in the UK PII: S0953-8984(97)80308-6

X-ray excited optical luminescence, photoluminescence, photostimulated luminescence and x-ray photoemission spectroscopy studies on BaFBr:Eu

N Subramanian†, R Kesavamoorthy†, K Govinda Rajan†, Mohammad Yousuf†, Santanu Bera‡ and S V Narasimhan‡

† Materials Science Division, Indira Gandhi Centre for Atomic Research, Kalpakkam 603 102, Tamilnadu, India

‡ Water and Steam Chemistry Laboratory, Bhabha Atomic Research Centre, Kalpakkam 603 102, Tamilnadu, India

Received 13 December 1996, in final form 24 February 1997

Abstract. The results of x-ray excited optical luminescence (XEOL), photoluminescence (PL), photostimulated luminescence (PSL) and x-ray photoemission spectroscopy (XPS) studies on the x-ray storage phosphor BaFBr:Eu are presented in this paper. Analyses of XEOL, PL and PSL spectra reveal features corresponding to the transitions from $4f^6\ 5d^1$ to $4f^7$ configurations in different site symmetries of Eu^{2+}. Increasing x-ray dose is seen to lead to a red shift in the maximum of the PL excitation spectrum for the 391 nm emission. The XEOL and XPS spectra do not show any signature of Eu^{3+} in the samples studied by us, directly raising doubts about the model of Takahashi *et al* in which Eu^{2+} is expected to ionize to Eu^{3+} upon x-ray irradiation and remain stable until photostimulation. XEOL and PSL experiments with simultaneous x-ray irradiation and He–Ne laser excitation as well as those with sequential x-ray irradiation and laser stimulation bring out the competition between the F centre population and depopulation rates. A time scale ∼1–2 s, possibly related to the process of production of the electron/hole traps themselves, during x-ray irradiation, is observed. Relaxation of these traps upon photostimulation is also seen.

1. Introduction

Barium fluorobromide activated with europium is being widely used as the constituent phosphor material in imaging screens for two-dimensional x-ray radiography [1–5]. This material possesses storage properties by virtue of defects present in it. Under x-ray irradiation, the halide ion vacancies (F^+ centres) trap electrons to form F centres. This is how the image is believed to be formed. Deexcitation of the trapped electrons using an appropriate stimulating radiation, 632.8 nm in this case, gives rise to photostimulated luminescence (PSL) at around 391 nm, corresponding to the $4f^6\ 5d^1$ to $4f^7$ transitions in Eu^{2+}. A number of papers in the literature are devoted to topics involving the details concerning the interaction of x-rays with the phosphor, the nature of the stored image and the excitation and deexcitation mechanisms [1, 4]. However, a unique mechanism has not been arrived at so far.

It is of interest to note that the XEOL technique, among other luminescence techniques, is by far the best in quantification of ultra-trace levels (∼0.002 ppm) of rare earth elements in a wide variety of matrices [6]. Further, the XEOL spectrum carries important details about

0953-8984/97/224769+12$19.50

the energy levels of the rare earths within the energy band gap of the matrix. Therefore, studies on BaFBr:Eu from the standpoint of XEOL, along with PL and PSL, can be expected to shed more light on the processes leading to PSL.

The present paper discusses the results of XEOL, PL, PSL and XPS studies made by us on BaFBr:Eu. Particular emphasis has been placed on the XEOL and PSL measurements performed with simultaneous x-ray irradiation and He–Ne laser excitation as well as those with sequential x-ray irradiation and laser stimulation. These studies are expected to bring out the competition between the rates of population and depopulation of F centres. New results have been obtained in our studies and, as far as possible, these are interpreted within the framework of the existing PSL mechanisms available for barium fluorohalides.

2. Experimental details

The BaFBr:Eu samples with 0.1 mol% of europium were prepared by direct solid state reaction between the individual halides in a nitrogen atmosphere. X-ray powder diffraction patterns indicated that the samples were essentially in a single phase. The patterns matched very well with the standard JCPDS data and could be indexed to the matlockite (PbFCl) structure adopted by BaFBr.

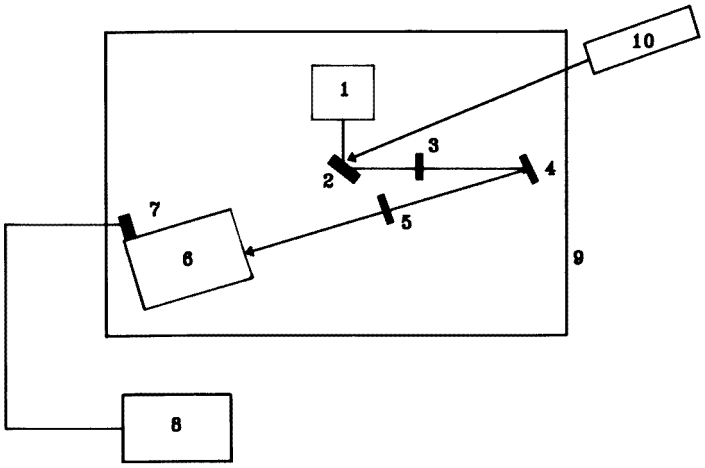

Figure 1. A schematic of the setup for XEOL and PSL studies: 1, rotating anode x-ray generator (RAXRG); 2, sample; 3, collecting lens; 4, mirror; 5, Focusing lens; 6, monochromator; 7, photomultiplier tube (PMT); 8, PC based monochromator controller unit and data acquisition system; 9, radiation enclosure; 10, He–Ne laser.

A simple facility for performing XEOL and PSL studies has been recently set up in our laboratory and is shown in figure 1. A white beam derived from a rotating anode x-ray generator (Rigaku; maximum power rating, 18 kVA, with long-term beam stability of better than 0.1%) serves as the excitation source for XEOL. Typical operating settings of 30 kV anode voltage and 100 mA filament current are found to yield good XEOL spectra.

A high-resolution optical monochromator (Jobin-Yvon, HR-320; 1200 lines mm^{-1} grating) is used to analyse the luminescence signal. The exit slit of the monochromator is coupled to a photomultiplier tube (PMT) operating at 600 V. Optical parts, including the monochromator, are all positioned in the configuration shown in figure 1 so as to contain them inside the radiation enclosure of the x-ray generator. A personal computer

based spectrometer control and data acquisition system (Jobin-Yvon, Spectralink) forms an integral part of the XEOL setup. An He–Ne laser (Melles-Griot; 10 mW; 632.8 nm) is used to stimulate the PSL process.

To optimize the optical alignment, the sample is first irradiated by x-rays and the luminescent spot is seen. The He–Ne laser beam is next made to be incident at the centre of the luminescent spot. The x-ray beam is then cut off and the optical arrangement is manipulated to maximize the counts detected by the PMT at the lasing wavelength. This kind of alignment enables XEOL and PSL experiments to be carried out in the coincidence and anticoincidence modes. The monochromator entrance slit width is set at 3 mm so as to obtain a reasonably good signal to noise ratio. The instrumental resolution at this slit width is $\sim$3.8 nm.

XEOL spectra have been recorded by step scanning the monochromator, with a typical step width of 0.2 nm and an integration time of 5 s for each step. The PSL intensity is recorded at each wavelength after allowing the x-ray irradiation of the sample for a sufficient time to saturate the XEOL signal and then shining the laser onto the sample. Here, the typical step size is $\sim$2 nm. Excitation and emission spectra corresponding to PL and PSL have been recorded using a spectrofluorometer (Shimadzu RF 5000; 150 W; CW xenon lamp source). The instrumental resolution has been set at $\sim$2.5 nm. XPS spectra have been recorded using an Al Kα x-ray as probe beam (Fisons, Esca Lab 200X) with the samples mounted on indium foil. Experiments have been done at two power levels of the source, namely, 0.1 kVA and 0.3 kVA.

3. Results and discussion

Figure 2 curve a shows the XEOL spectrum of BaFBr:Eu recorded in the region 360–460 nm at an x-ray power level of 3 kVA. This power level is equivalent to a radioactive source of a few millicuries strength. A broad band, centred at 391 nm, with humps located on the right shoulder is seen. Decomposition of this multiplet by fitting Gaussians (i.e., taking the luminescence intensity as a function of energy of the emitted light photons) revealed the presence of four peaks positioned at 391, 405, 412 and 420 nm with normalized intensities 100, 19, 10 and 8, and full width at half maximum (FWHM) 27.14, 10.62, 16.52 and 18.9 nm respectively. The fitted XEOL spectrum, obtained by summing the area under the four peaks, is shown as the continuous curve passing through the observed data points.

The 391 nm main band is associated with the well known interconfigurational transition from the $4f^6\ 5d^1$ to the $4f^7$ state of Eu^{2+}. The possibility that any of the remaining three peaks may arise from the intraconfigurational transitions of the $4f^7$ state can be ruled out from considerations of their large FWHMs. This is because intraconfigurational transitions are generally quite narrow (one to two orders of magnitude less than the interconfigurational transition lines) and are usually reasonably resolved at low temperatures only [7]. Nevertheless, a comparison with the XEOL spectrum of an undoped BaFBr sample shown in figure 2, curve b, reveals clearly that the multiplet structure corresponds to Eu^{2+} transitions only. The origin of these peaks remains to be understood. The possibility that all these peaks have their origin in the $4f^6\ 5d^1$ to $4f^7$ interconfigurational transitions in Eu^{2+} which are present in inequivalent sites cannot be ruled out.

Figure 3 curve a shows the PL excitation spectrum for 391 nm emission. Excitation wavelengths of 234 nm and 284 nm, indicated by arrows in figure 3, have been selected to record the emission spectra, depicted in figure 3 as curves b and c respectively. The multiplet structure akin to that observed in the XEOL spectrum, figure 2 curve a, is seen in figure 3 curve b also. The multiplet structure is, however, not quite evident from figure 3

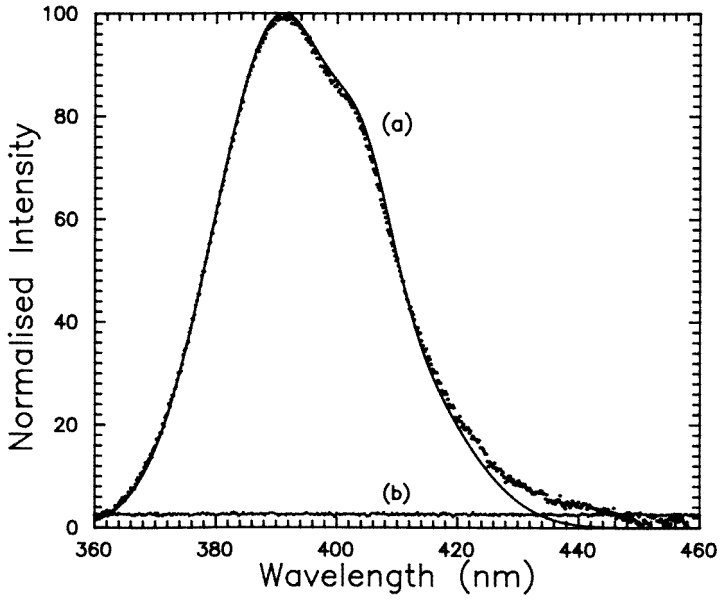

Figure 2. Curves a, the XEOL spectrum of BaFBr:Eu. The dotted curve is the observed spectrum and the continuous curve passing through the observed spectrum is the fitted spectrum. Curve b, the XEOL spectrum of pristine BaFBr.

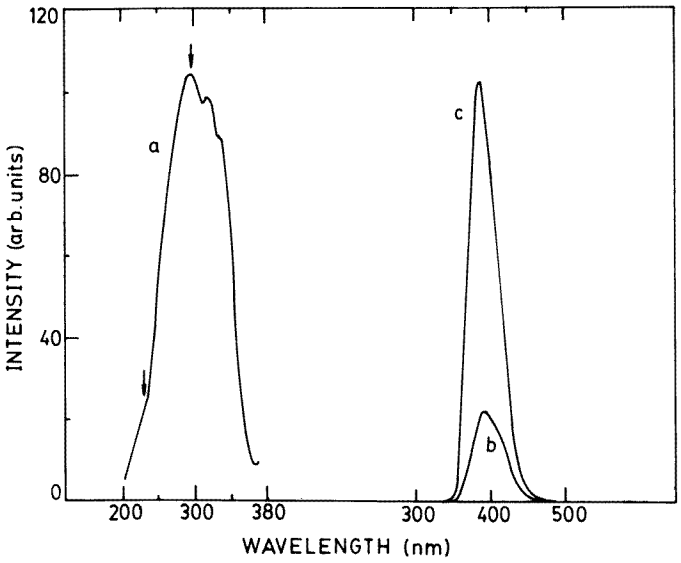

Figure 3. Curve a, the PL excitation spectrum for an emission wavelength of 391 nm; curve b, the PL emission spectrum for an excitation wavelength of 234 nm; curve c, the PL emission spectrum for an excitation wavelength of 284 nm.

curve c. Nevertheless, decomposition of a typical emission spectrum excited by 284 nm radiation (figure 4) gives four peaks positioned at the same wavelengths as those of the XEOL spectrum. Figure 4 shows also the fit to the observed PL spectrum obtained by

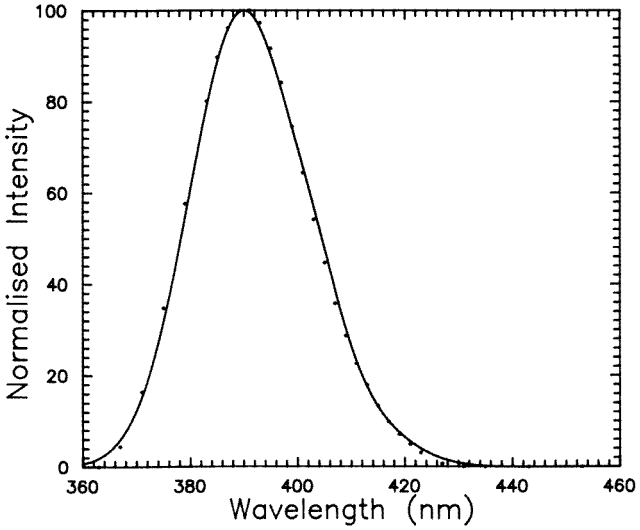

Figure 4. The PL emission spectrum for an excitation wavelength of 284 nm. The dots are the experimental points and the continuous curve passing through them is the fitted spectrum.

Table 1. Fitted parameters for XEOL, PL and PSL spectra of BaFBr:Eu.

Spectrum	λ (nm)	FWHM (nm)	Relative intensity
XEOL (figure 2 curve a)	391	27.14	100
	405	10.62	19
	412	16.52	10
	420	18.90	8
PL (figure 4)	391	24.31	100
	405	10.62	8
	412	14.16	4
	420	15.34	2.5
PSL (figure 8)	391	24.78	100
	405	10.62	28
	412	16.52	14
	420	18.88	13

adding the above four peaks. It can be noted that the fit is quite good. It is interesting to note that, although the peak positions and FWHMs are nearly the same in both XEOL and PL spectra, the relative intensities of the three PL subpeaks are rather lower than those in the case of XEOL. Table 1 summarizes the above results. It is not clear why, when excited by 234 nm wavelength the BaFBr:Eu sample emits the 391 nm PL band with a clear multiplet structure, whereas when excited by 284 nm wavelength the multiplet structure is not very obvious. In the forthcoming paragraph, the origin of the 284 nm (∼4.4 eV) absorption level of Eu^{2+} is discussed.

Both Takahashi *et al* [3, 5] and Rüter *et al* [8] have considered in their energy level schemes, the presence of an Eu^{2+} excited level at ∼4.6 eV above the $^8S_{7/2}$ level taking part in the PL process at 3.2 eV (∼390 nm). We observed that the PL excitation maximum

for 3.2 eV emission shifts to higher wavelengths as the x-ray dose is increased as shown in table 2. This can probably be understood if the level corresponding to the PL excitation maximum belongs to defect aggregates rather than to Eu^{2+}. That the defect aggregates are indeed formed is exemplified by our observation of yellow colouration of the samples after heavy x-ray irradiation, which could not be bleached either by an He–Ne laser or by direct exposure to bright sunlight lasting for 3 d. Figure 5 curve a shows the excitation spectrum for 391 nm emission in such a sample. The corresponding PL emission spectrum, figure 5 curve b, excited with 343 nm shows an intense broad peak at 466 nm, apart from the 391 nm multiplet which appears to be much weakened in intensity. However, in the XEOL spectrum (figure 6) of this sample only the 391 nm multiplet can be seen, with no indication of a peak at 466 nm. The PSL spectrum of this sample was similar to the XEOL spectrum.

Table 2. The x-ray dependence of the excitation wavelength for 391 nm emission in BaFBr:Eu.

Sample history	Excitation maximum for 391 nm emission	Remarks
1. As prepared	284 nm (4.37 eV)	Sample appears milky white
2. x-ray irradiated for 10 min at 2 kVA power	305 nm (4.07 eV)	Pale yellow colouration easily bleachable with the He–Ne laser or sunlight
3. x-ray irradiated for a few hours at 10 kVA power	343 nm (3.62 eV)	Yellow colouration not bleachable with the He–Ne laser or sunlight

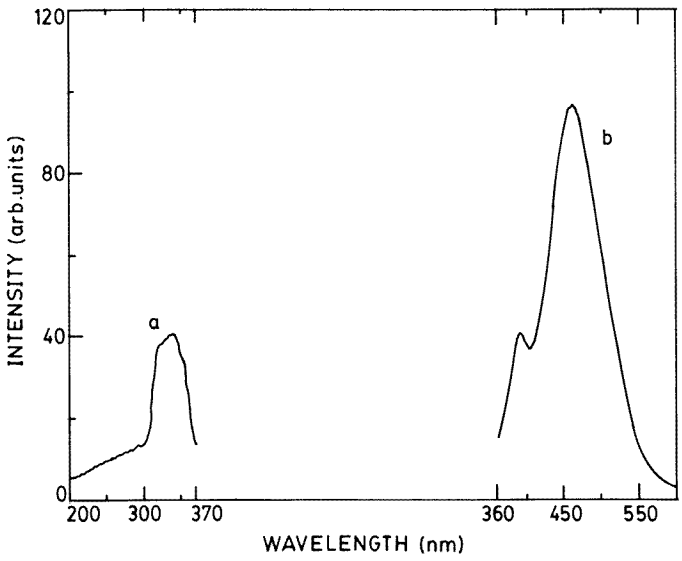

Figure 5. Curve a, the PL excitation spectrum of a heavily irradiated sample for an emission wavelength of 391 nm. Curve b, the PL emission spectrum of a heavily irradiated sample for an excitation wavelength of 343 nm.

This shows that in the PL experiment the 343 nm radiation effectively couples to an as yet unidentified defect species causing the 466 nm emission at the cost of 391 nm emission.

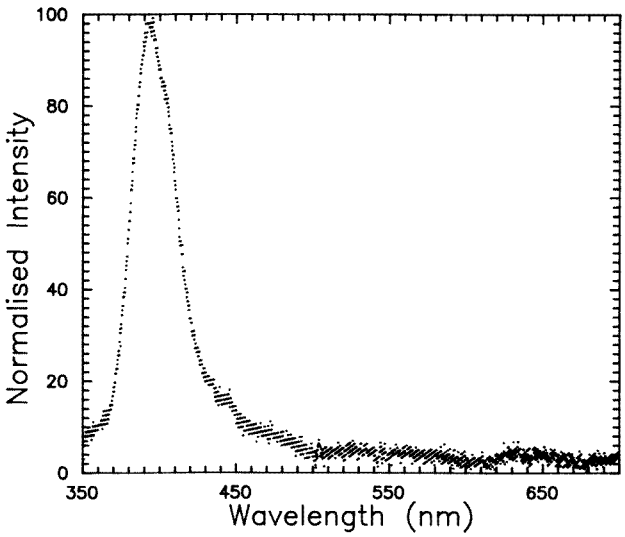

Figure 6. The XEOL spectrum of a heavily x-ray irradiated sample showing (i) that there is no indication of a peak at 466 nm in contrast to what is observed in the PL spectrum, figure 5 curve b, and (ii) the absence of Eu^{3+} signature at around 620 nm.

It may be pertinent to point out here that, in the literature, a peak has indeed been reported at this wavelength, in both doped and undoped BaFBr, and has been attributed to e^-–$V_k(Br_2^-)$ centres [8, 9].

Various models have been suggested regarding the mechanism of PSL in this phosphor. von Seggern *et al* [10] and Rüter *et al* [8] have proposed that under x-ray irradiation free excitons (e^-–h pairs) are produced, and these become trapped between adjacent halogen ions to form e^-–V_k centres. These e^-–V_k centres evolve into F–H pairs stabilized by the Eu^{2+} ions to form Eu^{2+}–F–H complexes. This is the stored image. On shining with 632.8 nm light, the trapped electrons are raised to the relaxed excited state (RES) of the F centres, from where they tunnel to the correlated Eu^{2+}–defect complex sites and destabilize them leaving excited $(H–e^-)^*$ pairs. These subsequently decay to $(e^-–V_k)^*$ pairs. The excited e^-–V_k pairs transfer their energy to the Eu^{2+} ions, leaving the latter in their excited state. Ultimately the 391 nm emission comes from the Eu^{2+*} to Eu^{2+} transition. X-ray excited luminescence studies on single crystals of undoped barium fluorohalides have indeed shown the formation of F–H pairs [9]. Apart from tunnelling from the RES, some of the electrons may be thermally lifted into the conduction band (CB) from the RES, which is ∼35 meV below the CB [8, 10]. Subsequently they can recombine at the spatially uncorrelated Eu^{2+}–hole centres accompanied by Eu^{2+} emission at 391 nm.

Takahashi *et al* [3, 5] have proposed a simple model which essentially requires ionization of Eu^{2+} to Eu^{3+} under x-ray irradiation and the transport of the liberated electrons via the CB to the traps. On stimulation with 632.8 nm, the trapped electrons are raised to the RES, ∼35 meV below the CB, from where these are thermally lifted onto the CB. Thereafter, these electrons recombine with the Eu^{3+}, producing Eu^{2+} in their excited state, which in turn make transitions to the ground state, causing emission of the 391 nm band. This mechanism, therefore, requires that the Eu^{3+} produced during the image storage process remains stable until it is converted back to Eu^{2+} after the electrons, stimulated out of the traps, recombine with it. If that is the case, it becomes relevant to address the question as to

whether one should expect interconversion between Eu^{2+} and Eu^{3+} during constant x-ray irradiation. However as can be seen in figure 6, the XEOL spectrum does not bear any signature of Eu^{3+} expected at ∼620 nm. This indicates that, even if Eu^{3+} is formed during x-ray irradiation, it is extremely unstable and recombines immediately with an electron, giving Eu^{2+*}.

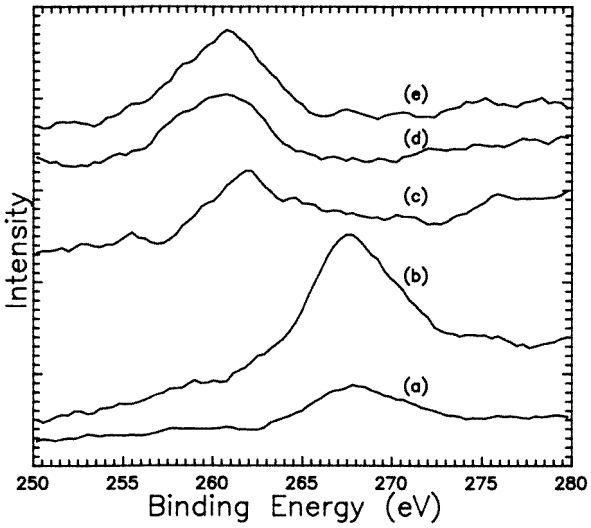

Figure 7. XPS spectra showing the Eu $4P_{3/2}$ peak for Eu_2O_3 (a), EuF_3 (b), EuS (c), BaFBr:Eu (Fuji) (d), and BaFBr:Eu (1 mol%, prepared by us) (e).

In order to unambiguously find the charge state of Eu in BaFBr, XPS experiments were performed taking Eu_2O_3, EuF_3 and EuS, in which Eu is present in the trivalent and divalent states, for comparison [11]. XPS was performed on both commercial (Fuji) and in-house prepared samples of BaFBr:Eu. Figure 7 shows the XPS results. On comparing the Eu $4P_{3/2}$ peak positions corresponding to the various samples, it can be inferred that Eu exists in BaFBr in the divalent state only. Even after prolonged exposure to x-rays, the Eu $4P_{3/2}$ peak of BaFBr:Eu neither shifted nor was distorted.

These XPS results, in conjunction with the absence of an Eu^{3+} signature in the XEOL spectra, indicate that Eu is present mainly in the 2+ charge state in the samples studied by us. The picture of Takahashi *et al* [3, 5] concerning the 3+ charge state of Eu in BaFBr during the image formation and storage process therefore seems untenable.

In fact, XEOL experiments performed by Sun and Su [12], on BaFBr samples in which both Eu^{2+} and Eu^{3+} coexist, have shown that under x-ray irradiation Eu^{2+} emission is enhanced owing to the *in situ* reduction of Eu^{3+} to Eu^{2+}. Also, their XEOL experiments on samples containing only Eu^{3+} reveal reduction from Eu^{3+} to Eu^{2+}. Further, according to them, the fraction of Eu^{2+} formed by reduction of Eu^{3+} is unstable and, after the luminescence process, captures holes and becomes once again Eu^{3+}. The cycle is as follows: $Eu^{3+} + e^- \rightarrow Eu^{3+}$ CTS (charge transfer state); $Eu^{3+}CTS \rightarrow Eu^{3+}CTS^* \rightarrow Eu^{2+*} + h$; $Eu^{2+*} \rightarrow Eu^{2+} + 391$ nm photon; $Eu^{2+} + h \rightarrow Eu^{3+}$.

Therefore, if our samples somehow had Eu^{3+} as a stable species (as in the case of the Takahashi picture) to begin with, then, during x-ray irradiation, during either XEOL or XPS measurement, one could expect a cyclic interconversion between the 2+ and 3+ states. This would lead to signatures of both the charge states in the XPS spectra and not simply

that of the 2+ state. This is, however, not what we observe. Hence, we tend to conclude that Eu^{3+} cannot be present as a stable entity in BaFBr during the image formation and storage process.

Recently, Dong and Su [13] have carried out careful time and temperature dependent Eu^{2+} luminescence (x-ray stimulated as well as photostimulated) and electroconductivity studies on BaFBr:Eu. They observed that the time and temperature dependences of the luminescence and electroconductivity were different. This was in total contrast to the results of similar experiments by Takahashi *et al* [3] and Iwabuchi *et al* [14, 15]. Thus they conclude that the Takahashi picture is questionable.

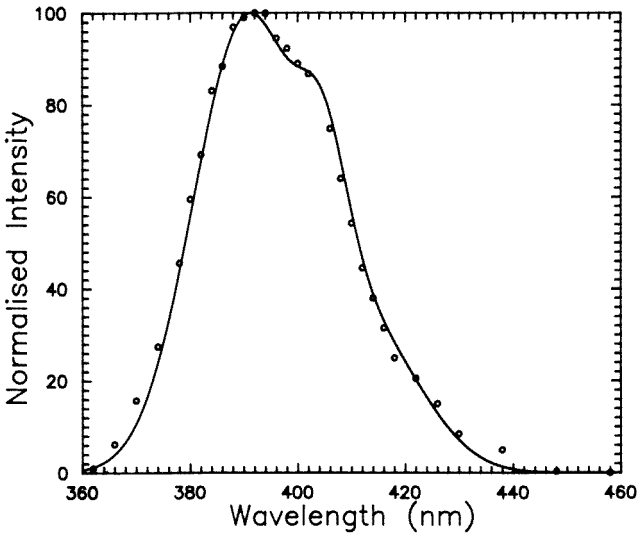

Figure 8. The PSL emission spectrum for a stimulation wavelength of 632.8 nm. Circles are the experimental points and the smooth curve passing through the observed spectrum is the fitted spectrum.

Figure 8 shows the PSL spectrum of the sample stimulated by a 632.8 nm He–Ne laser beam. This spectrum shows multiplet structure similar to that of XEOL. Table 1 shows the various fitted parameters corresponding to figure 8. It is noted that the peak positions of all the four components in the PSL multiplet are the same as those in the XEOL and the PL spectra. The width of the 391 nm peak is marginally reduced as compared to that in XEOL spectrum while those of the others remain unchanged. Also, the relative intensities are slightly different from those in XEOL.

It would be quite interesting to see the results of experiments in which XEOL and PSL can be studied simultaneously and sequentially. Such studies can be expected to throw light on the competing processes such as F centre population and depopulation rates. In these experiments, the monochromator grating has been set at the XEOL (or PSL) emission peak of 391 nm and the PMT signal intensity monitored while a series of temporal operations is performed. Figure 9 depicts this sequence of experiments, denoted as (I)–(VI).

(I) When the x-ray source is switched on, the XEOL signal is seen to rise sharply at first, followed by an exponential rise up to a saturation level 'SL'. This could be fitted to an equation of the type

$$I(t) = A(1 - e^{-Bt}).$$

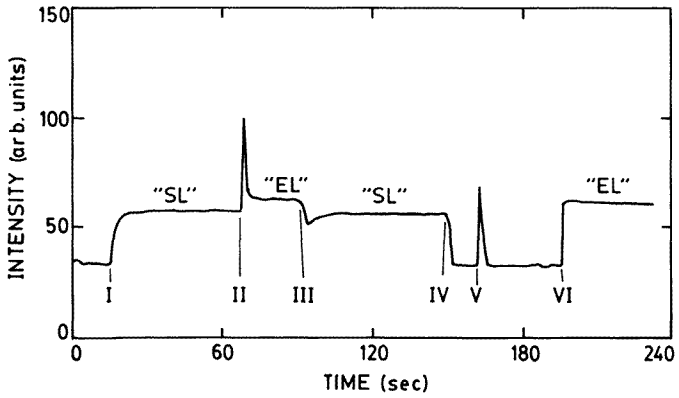

Figure 9. Intensity of 391 nm signal as a function of time; labels (I)–(VI) denote various temporal operations carried out (refer to text for a description).

The characteristic rate constant, B, for the XEOL intensity to build up to saturation is around 0.45 s^{-1}. The parameter A is found to be proportional to the x-ray intensity, unlike B.

(II) At the XEOL saturation level 'SL', the He–Ne laser is turned on. A sharp peak owing to the deexcitation of the trapped electrons constitutes the PSL signal. The intensity then reaches a new level 'EL', which is larger than 'SL'. We interpret 'EL' as arising due to XEOL and PSL occurring when a steady state is achieved between the population and the depopulation rates of the F centres.

(III) At 'EL', when the laser is cut off, the signal immediately falls, reaches a level discernibly below 'SL', and then is restored exponentially to 'SL'. The rate constant in this case is similar to the parameter B obtained earlier.

(IV) When the x-ray source is now switched off, the signal drops to the background.

(V) Shining the laser brings about the PSL (stored), where there is no appearance of features indicating competing processes in contrast to what was seen in the simultaneous x-irradiation and photostimulation experiment (step (III)). Hence, after depopulating all the PSL centres, the signal is restored to the background level.

The above study (steps (I)–(V)) clearly reveals that F centres are populated in the material by the incident x-ray photon flux at the cost of XEOL. Once all the traps are filled, the XEOL is restored to its original intensity ('SL'). That this is the case is also confirmed in the step (VI) of figure 9, where, with the laser still shining on the sample, when the x-ray source is switched on, the signal is seen to rise sharply to a level the same as 'EL'. This dynamic behaviour can be understood in terms of rate equations describing the various processes.

Another important piece of information that can be obtained from these experiments is the existence of a time scale of ∼1–2 s, apart from typical timescales of ∼microseconds. The latter are known to be associated with (i) the lifetime of the Eu ions in their excited state, (ii) the time taken for the transport of the photostimulated electrons to the sites of hole traps and recombination there and (iii) the time taken to fill the traps. Based on our observation (mentioned earlier) of formation of defect centres and their aggregates upon x-ray irradiation, we are led to believe that the larger time scale (∼1–2 s) is related to the much slower process of the production of traps themselves. Thus when the x-rays fall on the BaFBr:Eu sample, both processes, namely, filling up of traps by the generated electrons

and holes (the fast process) as well as formation of more traps (the slow process) occurs.

Step (III) of this experiment reveals a very interesting aspect related to the relaxation of a good fraction of the displaced ions to their original lattice positions (i.e., annihilation of the traps themselves) upon photostimulation. This is brought out clearly when the laser is cut off, whence the signal at 391 nm reaches a level well below 'SL' and then exponentially grows to 'SL' with the time scale of ∼1–2 s. In an indirect way, this experiment confirms the x-ray image storage in the form of defect complexes involving displacements of lattice ions, which relax to their original condition upon photostimulation. These complexes may be related to the Eu^{2+}–F–H defect complexes reported by von Seggern *et al* [10] and Rüter *et al* [8] to be formed during x-ray irradiation and destabilized upon photostimulation. This leads to a relaxation of the anions that had taken part in the H-centre formation during x-irradiation (and thereby having been displaced from their crystal lattice positions) to their parental lattice positions.

4. Summary

We have investigated the luminescence characteristics of BaFBr:Eu phosphor and the major findings are the following.

(i) The XEOL and XPS spectra do not show any signature of Eu^{3+} in the samples studied by us. This result is significant in the sense that it gives direct evidence that the Takahashi model of PSL process in BaFBr:Eu is questionable inasmuch as it considers the existence of Eu in a stable 3+ charge state after x-ray irradiation.

(ii) Detailed line shape analysis of the observed multiplet structure in the luminescence spectra indicates the necessity of considering the presence of Eu ions in various inequivalent sites.

(iii) Inspired by the observation that the excitation maximum for 391 nm emission shifts with the x-ray dose, we conjecture that the 4.6 eV level in the energy band model for BaFBr:Eu might be associated with a radiation induced defect centre and not with Eu^{2+}.

(iv) Simultaneous and sequential XEOL and PSL experiments reveal the competition between the two processes. Under x-ray irradiation, the PSL centres are preferentially populated as compared to the XEOL centres. A new time scale, ∼1–2 s, possibly related to the process of production of the electron traps themselves during x-ray irradiation, has been observed.

Acknowledgments

Authors acknowledge Dr P Ch Sahu, Shri N V Chandra Shekar, Shri M C Valsakumar, Dr K P N Murthy and Shri M Sekar for their help and valuable discussions. They also thank Shri B S Panigrahi for the PL measurements and discussions. They are thankful to Shri L Meenakshi Sundaram for various assistance. Finally they record their thanks to Fuji, Japan, for their gift of an imaging phosphor screen.

References

[1] Blasse G 1993 *Solid State Luminescence—Theory, Materials and Devices* ed A H Kitai (London: Chapman and Hall) ch 11, p 349 and references therein

[2] Sonoda M, Takano M, Miyahara J and Kato H 1983 *Radiology* **148** 833

[3] Takahashi K, Kohda K, Miyahara J, Kanemitsu Y, Amitani K and Shinoya S1984 *J. Lumin.* **31/32** 266

[4] Lakshmanan A R and Govinda Rajan K 1994 *Radiat. Prot. Dosim.* **55** 247
Govinda Rajan K, Mohammad Yousuf, Subramanian N, Kesavamoorthy R and Lakshmanan A R (eds) 1996 *Photostimulated Luminescence and its Applications* (New Delhi: Allied)
Klee R J 1995 *J. Phys. D: Appl. Phys.* **28** 2529
[5] Takahashi K, Shibahara Y and Miyahara J 1985 *J. Electrochem. Soc.* **132** 1492
[6] D'Silva A P and Fassel V A 1979 *Handbook on the Physics and Chemistry of Rare Earths* vol 4, ed K A Gschneidner Jr and L Eyring (Amsterdam: North-Holland) ch 37E p 441
[7] Brixner L H, Bierlein J D and Johnson V 1980 *Current Topics in Materials Science* vol 4, ed E Kaldis (Amsterdam: North-Holland) ch 2, p 47
[8] Rüter H H, v Seggern H, Reininger R and Saile V 1990 *Phys. Rev. Lett.* **65** 2438
[9] Crawford M K, Brixner L H and Somaiah K 1989 *J. Appl. Phys.* **66** 3758
[10] von Seggern H, Voight T, Knupfer W and Lange G 1988 *J. Appl. Phys.* **64** 1405
Thoms M, von Seggern H and Winnacker A 1991 *Phys. Rev.* B **44** 9240
[11] Subramanian N, Mohammad Yousuf, Govinda Rajan K, Vijay Kumar, Santanu Bera and Narasimhan S V 1995 *Solid State Phys.* (India) C **38** 231
[12] Sun X-P and Su M-Z 1988 *J. Lumin.* **40/41** 171
[13] Dong Y and Su M-Z 1995 *J. Lumin.* **65** 265
[14] Iwabuchi Y, Umemoto C, Takahashi K and Shionaya S 1991 *J. Lumin.* **48/49** 481
[15] Iwabuchi Y, Mori N, Takahashi K, Matsuda T and Shionaya S 1994 *Japan. J. Appl. Phys.* **33** 178